

# SkeletonAgent: An Agentic Interaction Framework for Skeleton-based Action Recognition

Hongda Liu<sup>1,2</sup>, Yunfan Liu<sup>2\*</sup>, Changlu Wang<sup>1,2</sup>, Yunlong Wang<sup>1</sup>, Zhenan Sun<sup>1\*</sup>

<sup>1</sup>NLPR, Institute of Automation, Chinese Academy of Sciences

<sup>2</sup>University of Chinese Academy of Sciences

{hongda.liu, changlu.wang, yunlong.wang}@cripac.ia.ac.cn

liuyunfan@ucas.ac.cn, znsun@nlpr.ia.ac.cn

## Abstract

Recent advances in skeleton-based action recognition increasingly leverage semantic priors from Large Language Models (LLMs) to enrich skeletal representations. However, the LLM is typically queried in isolation from the recognition model and receives no performance feedback. As a result, it often fails to deliver the targeted discriminative cues critical to distinguish similar actions. To overcome these limitations, we propose SkeletonAgent, a novel framework that bridges the recognition model and the LLM through two cooperative agents, *i.e.*, *Questioner* and *Selector*. Specifically, the *Questioner* identifies the most frequently confused classes and supplies them to the LLM as context for more targeted guidance. Conversely, the *Selector* parses the LLM’s response to extract precise joint-level constraints and feeds them back to the recognizer, enabling finer-grained cross-modal alignment. Comprehensive evaluations on five benchmarks, including NTU RGB+D, NTU RGB+D 120, Kinetics-Skeleton, FineGYM, and UAV-Human, demonstrate that SkeletonAgent consistently outperforms state-of-the-art benchmark methods. The code is available at <https://github.com/firework8/SkeletonAgent>.

## 1. Introduction

Skeleton-based action recognition has received sustained attention for its robustness in complex environments and computational efficiency [7, 35, 37]. Considering the skeletal structure, most approaches employ Graph Convolutional Networks (GCNs) to model inter-joint dependencies and capture spatiotemporal dynamics [48, 55]. Building on recent advances in Large Language Models (LLMs), a growing line of research seeks to enrich skeletal representations

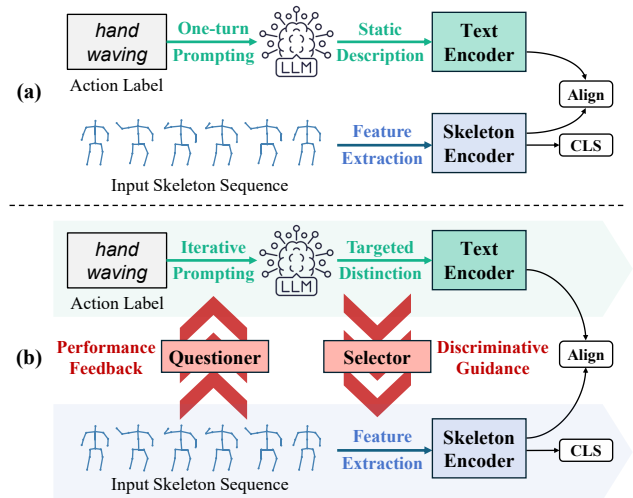


Figure 1. Comparison of (a) conventional multi-modal skeleton-based action recognition pipeline and (b) our SkeletonAgent. SkeletonAgent incorporates two cooperative agents, *i.e.*, *Questioner* and *Selector*, that create an interactive bridge to facilitate information flow between the action recognizer and the guidance provider (LLM), thereby narrowing the modality gap.

with multi-modal semantic priors, further enhancing the recognition accuracy [18, 21, 32, 43, 46, 57].

To be specific, these methods typically construct an associated space to bridge the modality gap between skeletal and textual semantics [32, 57]. As illustrated in Fig. 1 (a), they feed the LLM with prompts containing action labels, and then transform the generated descriptions into text features. The subsequent alignment establishes robust cross-modal relationships between these embeddings. Consequently, the language-derived vector enriches the skeletal representation with the LLM’s semantic priors.

Despite the remarkable progress, these multi-modal approaches still struggle to distinguish classes with similar joint trajectories (*i.e.*, *similar actions*). The core limita-

\*Corresponding authors.

tion lies in **the absence of an interactive feedback loop** between the action recognizer and the guidance provider (LLM). Concretely, this disconnect undermines discrimination in two ways: **(1) Homogeneous textual semantics.** For similar actions, the text descriptions produced by existing single-turn prompts are often semantically alike. This homogeneity conceals key discriminative cues, resulting in semantics that lack the class-specific nuances needed for accurate recognition. **(2) Coarse Cross-Modal Alignment.** Even if the text contains differences, the holistic aligning paradigm adopted by most methods lacks fine-grained control over the correspondence between textual fragments and specific motion patterns. This often misplaces skeletal features relative to their intended semantics, preventing recognition models from attending to subtle distinctions.

To address these limitations, we propose SkeletonAgent, a novel framework for skeleton-based action recognition. The core of SkeletonAgent lies in the interactive feedback mechanism between recognition models and language models. Inspired by recent advances in agents, we leverage this agent-based framework with online execution capabilities, providing the LLM with real-time performance feedback and steering the recognizer toward discriminative patterns.

Specifically, the interaction framework involves two bridging agent components, namely the *Questioner* and the *Selector*. As illustrated in Fig. 1 (b), the *Questioner* supplies the LLM with instantaneous context-aware feedback from recognition models (e.g., the current challenging actions), prompting the LLM to emphasize subtle class distinctions in its responses. Then, the *Selector* iteratively queries and summarizes critical joints and distinguishing characteristics in the conversation history, converting them into local constraints and global semantics that can be leveraged by recognition models. Unlike previous studies that seek static details in a single turn, our two agents engage in an iterative and adaptive collaboration with recognition models, enabling them to focus on more distinctive salient cues. Experimental results demonstrate that SkeletonAgent establishes new state-of-the-art performance, achieving 94.5% accuracy on the NTU RGB+D dataset and thereby validating the effectiveness of the proposed approach.

The main contributions are summarized as follows:

- We introduce SkeletonAgent, a novel agent-based framework that establishes the online interaction between the recognition model and LLM, enabling targeted guidance for fine-grained action discrimination.
- We design a bi-directional feedback mechanism, where two specialized agents collaborate to extract key distinctive cues, achieving precise cross-modal alignment.
- Extensive experiments demonstrate that SkeletonAgent consistently achieves state-of-the-art performance on five benchmarks, including NTU RGB+D, NTU RGB+D 120, Kinetics-Skeleton, FineGYM, and UAV-Human.

## 2. Related Work

### 2.1. Skeleton-based Action Recognition

Skeleton-based action recognition is to classify actions from sequences of estimated human key points. Early pioneering methods employ recurrent neural networks (RNNs) and convolutional neural networks (CNNs) to model the skeletons [8, 11, 20]. Following ST-GCN [48], the mainstream works in recent years have gradually focused on models based on Graph Convolutional Networks (GCNs) [1, 9, 25, 35, 52]. For instance, 2s-AGCN [35] introduces an adaptive framework that adaptively learns the graph topology between human joints. HD-GCN [19] leverages the hierarchically decomposed mechanism to identify the significant spatial relationships. Hyper-GCN [56] proposes an adaptive hyper-graph architecture to enhance the semantic aggregation of skeleton vertices. In addition, with the popularity of vision transformer, transformer-based methods have also been investigated for skeleton data [7, 42].

Despite these advances, existing methods remain largely uni-modal, lacking semantic guidance to distinguish fine-grained motions. In contrast, we introduce an online multi-modal training paradigm that leverages LLMs to provide context-aware discriminative cues. Through the evolving interaction process, our method achieves fine-grained alignment to improve the skeletal representations.

### 2.2. LLM Agents

An agent is defined as an entity that makes decisions and executes tasks in a dynamic, real-time environment to achieve specific goals. Recent advances in LLMs, particularly their emerging reasoning and planning capabilities [36, 53], have inspired recent research in natural language processing to leverage agents for complex tasks. The integration of chain-of-thought reasoning and self-correction could further extend the functionalities of LLMs [41]. These agent-based approaches have achieved notable success across various scenarios, such as prompt engineering, online search, and tool utilization [2, 50]. Simultaneously, the vision community has also adopted LLM agents for tasks like long video understanding and text-to-image generation [23, 40, 49].

Concretely, a key strength of LLM agents is their interactive capability, *i.e.*, the ability to process and utilize information across the real-time environment to make informed decisions. Inspired by this perspective, we propose SkeletonAgent, a novel framework that departs from prior methods by explicitly modeling the interactive relationship between recognition models and language models. Our agents enable dynamic interactions that progressively refine discriminative skeletal representations. Through this structured collaboration and selective inspiration, our method could achieve fine-grained discrimination.

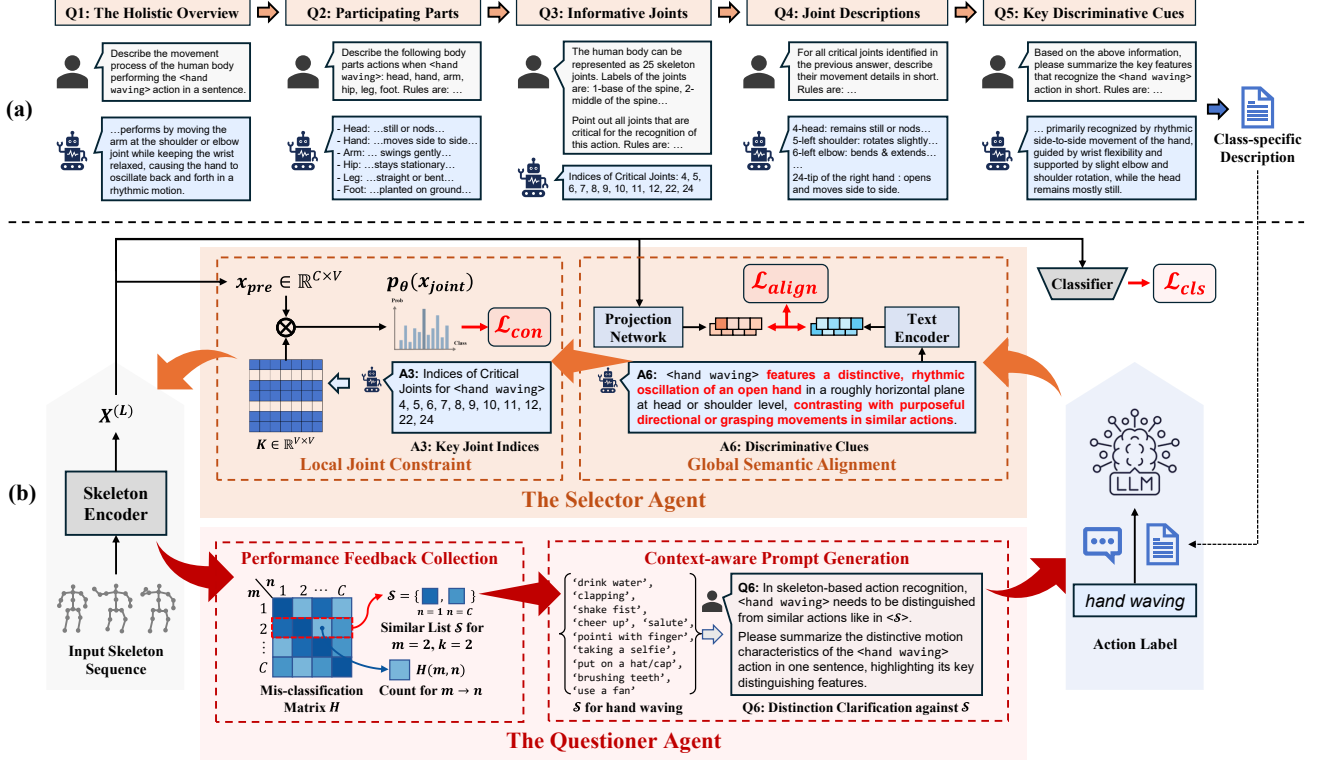


Figure 2. Illustration of (a) the generation pipeline of class-specific description, and (b) the overall framework of SkeletonAgent.

## 2.3. Multi-modal Representation Learning

Recent advances in language models have greatly accelerated progress in multi-modal representation learning. Methods such as CLIP [31] and ALIGN [15] demonstrate that vision-language training can learn robust representations for downstream tasks. For example, ActionCLIP [39] follows this training scheme and extends alignment to the video domain for action recognition. Beyond vision and language, ULIP [47] learns a unified representation space incorporating point clouds to improve understanding. Similarly, MotionCLIP [38] aligns human motion manifolds with CLIP latent space for human action generation. In the skeleton-based action recognition task, GAP [43] introduces generative prompts and a multi-part contrastive loss to align skeleton sequences with textual descriptions. Additionally, LA-GCN [46] constructs semantic-aware graph topologies derived from text to model joint relationships.

However, these methods rely on static text descriptions, which are often homogeneous across similar actions and lack fine-grained control over alignment. In contrast, our framework addresses this via the dynamic interaction mechanism. The proposed Questioner generates targeted distinctions based on recognition feedback, while the Selector injects salient joints and semantics into the model, enabling precise and adaptive cross-modal alignment.

## 3. Method

In this section, we introduce SkeletonAgent, a novel interaction framework for skeleton-based action recognition. We first briefly formalize the task and establish notation, followed by an overview of the architecture. Then, we detail the motivation and implementation of the two interactive agents, *i.e.*, the *Questioner* and the *Selector*. A schematic overview of SkeletonAgent is provided in Fig. 2.

### 3.1. Preliminaries

For skeleton-based action recognition, an input sequence with  $T$  frames is expressed as a tensor  $\mathbf{X} \in \mathbb{R}^{C \times T \times V}$ , where  $V$  denotes the number of joints and  $C$  denotes the latent dimension. Due to its inherent structural characteristics, the graph-like human skeleton is usually processed with GCNs. Let  $\mathbf{X}^{(l)}$  be the feature at the  $l$ -th layer, the graph convolution can be formulated as

$$\mathbf{X}^{(l)} = \sigma(\mathbf{D}^{-\frac{1}{2}} \mathbf{A}^{(l)} \mathbf{D}^{\frac{1}{2}} \mathbf{X}^{(l-1)} \mathbf{W}^{(l)}) \quad (1)$$

where  $\mathbf{A}$  is the adjacency matrix representing joint connectivity,  $\mathbf{D} \in \mathbb{R}^{N \times N}$  is the normalized degree matrix,  $\mathbf{W}^{(l)}$  denotes the learnable parameter of the  $l$ -th layer, and  $\sigma$  indicates the ReLU activation function. With a network comprising  $L$  layers with parameters  $\theta$ , the final feature  $\mathbf{X}^{(L)}$  is

passed to a classifier that produces one-hot encoding, which is trained using the cross-entropy loss  $\mathcal{L}_{cls}$  as follows

$$\mathcal{L}_{cls} = -\mathbf{y} \log \mathbf{p}_\theta(\mathbf{x}) \quad (2)$$

where  $\mathbf{y}$  is the one-hot ground-truth action label, and  $\mathbf{p}_\theta(\mathbf{x})$  denotes the predicted probability distribution.

### 3.2. Architecture Overview

The proposed SkeletonAgent establishes the dynamic interaction between the action recognizer and language models. As shown in Fig. 2, the framework consists of two cooperative agents. The Questioner monitors recognition performance and generates context-aware prompts that highlight distinctions between easily confused actions. Additionally, the Selector filters the multi-turn responses, extracting salient joints and discriminative cues that are injected into the model through local joint constraints and global semantic alignment. This agent-based interaction pipeline transforms targeted textual priors into training-aware guidance, enabling fine-grained action discrimination.

### 3.3. Questioner: A Context-aware Prompter

Existing methods typically query the LLM with the single-turn static prompt, which often yields nearly identical descriptions for similar actions. To tackle this issue, SkeletonAgent augments this paradigm with a Questioner module.

Specifically, the Questioner provides the LLM with a coarse-to-fine prompt chain to obtain an initial class-specific description for each action. Then, the agent periodically profiles the class-wise recognition performance and identifies those hard-to-distinguish classes during training. Accordingly, it constructs targeted prompts that guide the LLM toward context-aware discriminative outputs.

**Class-specific Description Preparation.** As shown in Fig. 2 (a), SkeletonAgent initially asks the LLM to describe the intrinsic characteristics of each action class. In practice, human tends to build a global understanding of the action, then curiously zoom in to explore specific joints in greater detail. Inspired by this human perceptual routine, we design a coarse-to-fine prompting sequence that first requests a holistic overview of the motion, then successively focuses on the participating body parts, the most informative joints, and finally the key discriminative cues.

Compared to existing studies, our step-wise prompt chain can yield richer and more informative skeleton-based descriptions. The complete prompts and sample responses construct the detailed class-specific descriptions for initial action perception, facilitating subsequent interactions.

**Performance Feedback Collection.** Our target is to establish the interactive mechanism between recognition models and language models. Therefore, we need to collect the real-time recognition feedback as guiding signals.

<b>Previous Static Description</b>
He is a tall man with dark hair and eyes. He is wearing a blue shirt and jeans. He is waving his hand in the air. Head nodding; hand waving; arm swinging; hip swaying; leg shifting; foot stomping.
<b>Questioner</b>
<b>Stage 1: Class-specific Context</b>
The hand waving action is primarily recognized by rhythmic side-to-side movement of the hand, guided by wrist flexibility and supported by slight elbow and shoulder rotation, while the head remains mostly still.
<b>Stage 2: Targeted Distinction</b>
Hand waving features a distinctive, rhythmic oscillation of an open hand in a roughly horizontal plane at head or shoulder level, contrasting with purposeful directional or grasping movements in similar actions.

Figure 3. Comparisons of previous static descriptions and the targeted distinctions provided by the Questioner. The proposed approach captures key distinctive cues and clearly differentiates them from the features of similar actions.

In practice, we maintain an online confusion matrix  $\mathbf{H}(\cdot; t)$  to identify the current challenging actions for each class (*i.e.*, similar-class set) at epoch  $t$ . Specifically, the  $(m, n)$ -th entry denoted as  $\mathbf{H}(m, n; t)$ , counts the samples of class  $m$  that are misclassified as belonging to class  $n$ . Here,  $m, n \in \{1, \dots, N_c\}$ , and  $N_c$  is the total number of action classes. Therefore, we define the similar-class set for class  $m$  as the  $k$  classes with the highest mis-classification counts in the current epoch

$$\mathcal{S}_k(m) = \{n \mid n \in \text{Top}_k(\mathbf{H}(m, \cdot))\} \quad (3)$$

where  $\text{Top}_k(\mathbf{H}(m, \cdot))$  returns the indices of the  $k$  largest entries in the  $m$ -th row of the mis-classification matrix  $\mathbf{H}$ . Essentially,  $\mathcal{S}_k(\cdot)$  captures the most confusable actions for each class. Consequently, the collected performance feedback can provide more valuable contextual information for training in subsequent epochs.

**Context-aware Prompt Generation.** After constructing the similar list  $\mathcal{S}$ , we pass the current challenging actions of each class to the LLM via the targeted prompt shown in Fig. 2 (b). This context-aware profile serves to encourage the LLM to focus on the subtle motion cues that distinguish the mentioned class from its most easily confused actions, thereby highlighting its targeted distinctive characteristics in the corresponding responses.

According to the results in Fig. 3, the static description from GAP [43] reflects the lack of fine-grained information on key characteristics for the *hand waving* action. In contrast, our approach can capture more salient cues and clearly differentiate them from similar actions. In addition, this interaction is carried out iteratively throughout training,

progressively increasing inter-class separability in the joint skeleton–text feature space. In this way, the Questioner supplements the class-specific descriptions with this class-wise confusion profile, thereby providing the LLM with explicit feedback on inter-class ambiguities.

### 3.4. Selector: An Adaptive Knowledge Highlighter

The previous holistic aligning paradigm lacks the fine-grained control over the correspondence between textual fragments and motion patterns. Meanwhile, the interactive mechanisms introduce more descriptions, where the truly informative knowledge needs to be refined to enable recognition models to comprehend these guidance cues.

Therefore, we propose the Selector agent that iteratively summarizes critical joints and distinguishing characteristics in the conversation history. The module converts the key information into local joint constraints and global semantic alignment that can be leveraged by recognition models.

**Local Joint Constraints.** By parsing the LLM’s answer, the joints and body parts most salient for action recognition can be readily identified. This information is injected into the recognition model through an auxiliary topology matrix  $\mathbf{K} \in \mathbb{R}^{V \times V}$ , which serves as an explicit structural constraint. Specifically,  $\mathbf{K}$  is initialized to zeros, and for each joint  $v$  identified as salient, the entire row  $\mathbf{K}(v, \cdot)$  is set to ones, effectively broadcasting that joint’s influence to all others. As the interaction proceeds, the matrix can be iteratively updated to reflect the latest set of salient joints, allowing the constraint to evolve together with the model.

To incorporate the matrix  $\mathbf{K}$  into the recognition pipeline, we first pool the final output of the network, *i.e.*,  $\mathbf{X}^{(L)} \in \mathbb{R}^{C \times T \times V}$ , along the temporal dimension  $T$ , yielding a preliminary joint–level representation  $\mathbf{x}_{\text{pre}} \in \mathbb{R}^{C \times V}$ . Afterward, the skeleton feature with critical joints emphasized, denoted as  $\mathbf{x}_{\text{joint}}$ , is obtained through

$$\mathbf{x}_{\text{joint}} = \text{Proj}(\mathbf{x}_{\text{pre}} \cdot \mathbf{K}) \quad (4)$$

where  $\text{Proj}(\cdot)$  is the projection operation consisting of a convolutional layer followed by reshaping. To make the encoder attend more strongly to these highlighted joints, we add the explicit constraint loss

$$\mathcal{L}_{\text{con}} = -\mathbf{y} \log \mathbf{p}_{\theta}(\mathbf{x}_{\text{joint}}) \quad (5)$$

where  $\mathbf{y}$  is the one-hot ground-truth label, and  $\mathbf{p}_{\theta}(\mathbf{x}_{\text{joint}})$  denotes the predicted class distribution. This supervision directs the model to exploit the injected joint priors, thereby learning more discriminative representations.

**Global Semantics Alignment.** In addition to the explicit joint-level constraint, we employ the global semantic alignment. Unlike previous methods that pair the skeletal representation with a generic context-agnostic description, we align it with the embedding of the Q6 response in Fig. 2 (b),

*i.e.*, text deliberately crafted to distinguish the target action from its most confusable counterparts.

Specifically, we adopt a bi-directional matching scheme to enhance the semantic alignment of the embeddings of skeleton and text. We employ the pre-trained CLIP model [31] as the text encoder. The above action descriptions are input into the encoder, undergoing standard tokenization and transformation to yield the corresponding textual features. Then, we define two probability distributions  $\mathbf{p}_i^{\text{s}2\text{t}}$  and  $\mathbf{p}_i^{\text{t}2\text{s}}$ , which represent the transition probabilities in skeleton-to-text and text-to-skeleton directions:

$$\mathbf{p}_i^{\text{s}2\text{t}}(\mathbf{s}_i) = \frac{\exp(\cos(\mathbf{s}_i, \mathbf{t}_i)/\tau)}{\sum_{j \in \mathcal{B}} \exp(\cos(\mathbf{s}_i, \mathbf{t}_j)/\tau)} \quad (6)$$

$$\mathbf{p}_i^{\text{t}2\text{s}}(\mathbf{t}_i) = \frac{\exp(\cos(\mathbf{t}_i, \mathbf{s}_i)/\tau)}{\sum_{j \in \mathcal{B}} \exp(\cos(\mathbf{t}_i, \mathbf{s}_j)/\tau)} \quad (7)$$

Here,  $\mathcal{B}$  is the batch size,  $i, j$  are the index of samples within the batch,  $\cos(\cdot)$  represents the cosine similarity,  $\tau$  is temperature parameter, and  $\mathbf{s}, \mathbf{t}$  represent the skeletal and textual representations obtained from the skeleton encoder and pre-trained text encoder, respectively.

Considering that multiple skeleton samples correspond to the same class, there could be more than one positive pair within the same batch. Therefore, we use KL divergence to measure the probability distributions between skeletal features and textual features, and the overall alignment loss  $\mathcal{L}_{\text{align}}$  can be written as

$$\mathcal{L}_{\text{align}} = \frac{1}{2} (KL(\mathbf{p}^{\text{s}2\text{t}}(\mathbf{s}), \mathbf{q}^{\text{s}2\text{t}}) + KL(\mathbf{p}^{\text{t}2\text{s}}(\mathbf{t}), \mathbf{q}^{\text{t}2\text{s}})) \quad (8)$$

where  $\mathbf{q}^{\text{s}2\text{t}}$  and  $\mathbf{q}^{\text{t}2\text{s}}$  represent the ground-truth probability distributions, with the positive pair probability set to 1 and the negative pair probability set to 0. Through this targeted semantic guidance, the recognition model can focus more on the key discriminative basis, thereby enhancing the synergistic skeleton-semantic relationships.

Finally, the overall loss function for training SkeletonAgent can be written as

$$\mathcal{L} = \mathcal{L}_{\text{cls}} + \alpha \mathcal{L}_{\text{con}} + \beta \mathcal{L}_{\text{align}} \quad (9)$$

where  $\mathcal{L}_{\text{cls}}$  is the cross-entropy loss used to supervise the classification, and  $\alpha, \beta$  are the weighting parameters to balance the importance of different loss terms.

## 4. Experiments

### 4.1. Datasets

**NTU RGB+D (NTU-60)** [33] is a large-scale human action recognition dataset that contains 56,880 indoor captured skeleton action samples, performed by 40 different subjects and classified into 60 classes. Each action sample is annotated with 25 skeleton joints and contains up to two

Table 1. Performance comparisons against state-of-the-art methods on the NTU RGB+D, NTU RGB+D 120, Kinetics-Skeleton, and FineGYM datasets in terms of classification accuracy (%).

Methods	Publication	NTU RGB+D		NTU RGB+D 120		Kinetics-Skeleton		FineGYM
		X-Sub	X-View	X-Sub	X-Set	Top-1	Top-5	Top-1
ST-GCN [48]	AAAI 2018	81.5	88.3	70.7	73.2	30.7	52.8	86.7
2s-AGCN [35]	CVPR 2019	88.5	95.1	82.5	84.2	36.1	58.7	-
MS-G3D [29]	CVPR 2020	91.5	96.2	86.9	88.4	38.0	60.9	92.0
MST-GCN [4]	AAAI 2021	91.5	96.6	87.5	88.8	38.1	60.8	-
CTR-GCN [3]	ICCV 2021	92.4	96.8	88.9	90.6	-	-	91.9
STF [17]	AAAI 2022	92.5	96.9	88.9	89.9	39.9	-	-
InfoGCN [6]	CVPR 2022	93.0	97.1	89.8	91.2	-	-	92.0
PYSKL [10]	ACM MM 2022	92.6	97.4	88.6	90.8	49.1	-	94.1
FR-Head [54]	CVPR 2023	92.8	96.8	89.5	90.9	-	-	-
UPS [12]	CVPR 2023	92.6	97.0	89.3	91.1	40.5	63.3	-
GAP [43]	ICCV 2023	92.9	97.0	89.9	91.1	-	-	-
HD-GCN [19]	ICCV 2023	93.4	97.2	90.1	91.6	40.9	63.5	94.6
Skeleton MixFormer [45]	ACM MM 2023	93.2	97.2	90.2	91.5	-	-	-
DS-GCN [44]	AAAI 2024	93.1	97.5	89.2	91.1	50.6	-	93.4
BlockGCN [55]	CVPR 2024	93.1	97.0	90.3	91.5	-	-	94.5
SkateFormer [7]	ECCV 2024	93.5	97.8	89.8	91.4	-	-	-
ProtoGCN [25]	CVPR 2025	93.8	97.8	90.9	92.2	51.9	75.6	95.9
Hyper-GCN [56]	ICCV 2025	93.7	97.8	90.9	92.0	-	-	-
Ours (2-ensemble)		94.0	97.7	90.5	92.4	52.2	75.9	96.1
Ours (4-ensemble)		94.3	98.0	91.4	93.0	53.0	76.8	96.4
<b>Ours (6-ensemble)</b>		<b>94.5</b>	<b>98.2</b>	<b>91.7</b>	<b>93.1</b>	<b>53.6</b>	<b>77.0</b>	<b>96.5</b>

subjects. This dataset recommends two evaluation protocols: (1) cross-subject (X-Sub): train data are performed by 20 subjects, and test data are performed by the remaining 20 subjects. (2) cross-view (X-View): train data from camera views 2 and 3, and test data from camera view 1.

**NTU RGB+D 120 (NTU-120)** [26] is an extended version of NTU RGB+D, and contains 114,480 skeleton action samples over 120 classes. The sequences are captured with 106 human subjects and 32 distinct camera setups. There are also two recommended settings: (1) cross-subject (X-sub): skeleton samples from 53 subjects are used for training, while the remaining 53 subjects are used for testing. (2) cross-setup (X-set): train data comes from 16 even setup IDs, and test data comes from 16 odd setup IDs.

**Kinetics-Skeleton** [16] is derived from the Kinetics 400 video dataset, utilizing the pose estimation toolbox to extract 240,436 training samples and 19,796 evaluation skeleton samples across 400 classes. For each sequence, two people are selected for multi-person clips based on the average joint confidence. We adopt the available data provided by PYSKL [10]. Following the standard evaluation protocol, the Top-1 and Top-5 accuracies are reported.

**FineGYM** [34] is a fine-grained action recognition dataset with 29,000 videos of 99 gymnastic action classes. Since the dataset contains diverse fine-grained actions, it requires recognition models to distinguish different sub-actions within the same video. This poses greater chal-

lenges to current recognition methods. We use the skeleton data provided by PYSKL [10]. The mean class Top-1 accuracy is reported in the evaluation protocol.

**UAV-Human** [22] is a large-scale human behavior understanding dataset with unmanned aerial vehicles, containing 155 classes from 119 subjects. The data are captured by drones in diverse environments. It defines two evaluation protocols: (1) cross-subject-v1 (CSv1) and cross-subject-v2 (CSv2), with 89 subjects for training and 30 for testing. The subject IDs are different across protocols. The classification accuracy is used for performance evaluation.

## 4.2. Implementation Details

Our implementation is conducted on a single RTX 3090 GPU with PyTorch. We employ PYSKL [10] as the skeleton extractor baseline. For the text encoder, we employ the pre-trained ViT-B/32 model of CLIP [31] to extract semantic embeddings. Concurrently, GPT-4o [14] is utilized to generate interactive dialogues. The model is trained for 150 epochs with the batch size set to 64. The initial learning rate is set to 0.1 with a cosine learning rate scheduler. The optimizer is SGD with a Nesterov momentum of 0.9 and a weight decay of  $5 \times 10^{-4}$ . The temperature  $\tau$  is set to 0.1, and the upper threshold  $k$  for class statistics is set to 10. The weights  $\alpha$  and  $\beta$  are set to 0.2 and 0.5. We sample the skeleton sequences to 100 frames and follow the strategy used in [3, 10, 51] for data preprocessing.

Table 2. Performance comparisons against state-of-the-art methods on UAV-Human in terms of classification accuracy (%).

Methods	Year	UAV-Human	
		CSv1	CSv2
Shift-GCN [5]	2020	38.0	67.0
FR-AGCN [13]	2022	44.0	69.5
TD-GCN [27]	2023	45.4	72.9
Skeleton MixFormer [45]	2023	48.9	74.2
HDBN [28]	2024	48.0	75.4
AL-GCN [30]	2024	48.8	74.0
TDSN-GCN [24]	2025	47.8	74.2
<b>Ours</b>		<b>52.1</b>	<b>78.1</b>

Table 3. Ablation study on the contribution of each component in SkeletonAgent under the NTU-60 X-Sub setting.

Baseline	Questioner		Selector		Acc (%)
	CSP	CAG	$\mathcal{L}_{con}$	$\mathcal{L}_{align}$	
✓	–	–	–	–	91.2
✓	✓	–	–	–	91.5
✓	✓	✓	–	–	92.0
✓	✓	✓	✓	–	92.3
✓	✓	✓	–	✓	92.6
✓	✓	✓	✓	✓	<b>92.8</b>

Table 4. Comparison of classification accuracies (%) based on (left) existing multi-modal methods and (right) different LLMs.

Methods	Acc (%)	LLMs	Acc (%)
Baseline	91.2	Gemini 2.5	92.2
w/ LA-GCN [46]	91.4	Claude Sonnet 4	92.5
w/ GAP [43]	91.3	GPT-5	92.6
w/ PURLS [57]	91.6	DeepSeek-V3.1	92.6
<b>Ours</b>	<b>92.8</b>	<b>GPT-4o</b>	<b>92.8</b>

### 4.3. Comparison with State-of-the-Art Methods

We compare ours with the state-of-the-art methods on five datasets, including NTU RGB+D, NTU RGB+D 120, Kinetics-Skeleton, FineGYM, and UAV-Human. Following InfoGCN [6], we adopt the six-stream ensemble strategy to report the results. As shown in Tab. 1 and Tab. 2, our model consistently establishes state-of-the-art performance with a significant margin in all scenarios. On the NTU-60 dataset, the model achieves the best accuracy of 94.5% on X-Sub and 98.2% on X-View. Remarkably, our model excels in performance on the challenging NTU-120 dataset, surpassing the performance of Hyper-GCN [56] by 0.8% on X-Sub and 1.1% on X-Set. As for Kinetics, SkeletonAgent outperforms state-of-the-art method ProtoGCN [25] by 1.7%. In addition, our model achieves state-of-the-art performance

Table 5. Comparison of classification accuracies (%) on three subsets for NTU-60 dataset and four challenging action classes.

	CTR-GCN	FR-Head	ProtoGCN	Ours
	[3]	[54]	[25]	
NTU-60 Hard	65.1	66.8	69.6	<b>73.9</b> <sup>+4.3</sup>
NTU-60 Medium	83.0	83.4	85.1	<b>87.6</b> <sup>+2.5</sup>
NTU-60 Easy	95.1	95.6	95.9	<b>96.6</b> <sup>+0.7</sup>
Play with phone	69.1	73.8	75.3	<b>78.2</b> <sup>+2.9</sup>
Writing	56.6	59.2	63.2	<b>68.0</b> <sup>+4.8</sup>
Wear a shoe	79.5	78.8	85.7	<b>93.4</b> <sup>+7.7</sup>
Take off a shoe	75.6	77.7	83.8	<b>88.3</b> <sup>+4.5</sup>

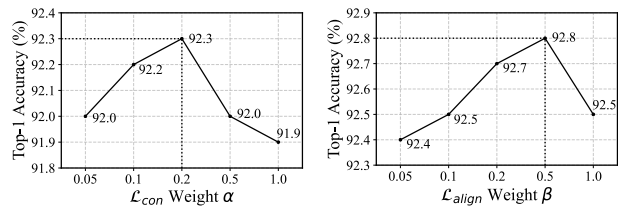


Figure 4. Ablation study on the influences of the weights  $\alpha$  and  $\beta$  under the NTU-60 X-Sub setting with the joint modality.

with a large margin on the fine-grained dataset FineGYM. This further confirms the efficacy of our approach for fine-grained action discrimination. According to the results in Table 2, the significant improvement of the proposed SkeletonAgent on the UAV-Human dataset demonstrates its powerful ability to model diverse and complex actions. Experimental results demonstrate the superiority of our method.

### 4.4. Ablation Study

We conduct ablation studies under the X-Sub setting of NTU-60 with the joint modality. In addition, we provide more experimental results in the supplementary materials.

**Effectiveness of Each Module.** To verify the effectiveness of SkeletonAgent, we gradually add each component to conduct comparative experiments in Tab. 3. For the Questioner agent, we observe a performance improvement of 0.3% with the Class-Specific Preparation (CSP). Building upon the contextual dialogues provided by the Context-Aware Generation (CAG) improves performance by 0.5%. Subsequently, we examine the explicit constraint  $\mathcal{L}_{con}$  and semantics alignment  $\mathcal{L}_{align}$  of the Selector agent, achieving performance improvements by 0.3% and 0.6%, respectively. This indicates that dynamic interactions facilitated by agents contribute to enhancing the skeletal discriminative representations. By integrating all components, we surpass baseline performance by 1.6%, which demonstrates the effectiveness of the proposed framework.

**Effectiveness of Contextual Interaction.** To examine the efficacy of the dynamic interaction mechanism, we conduct the analysis between the proposed SkeletonAgent and

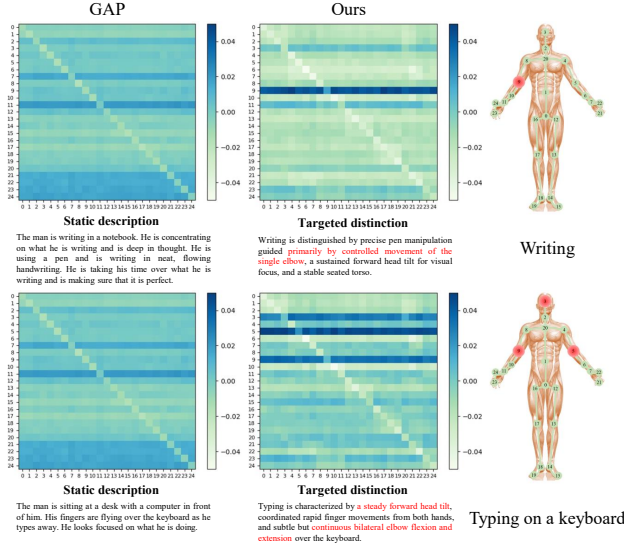


Figure 5. Visualization of action descriptions and the topologies learned by GAP [43] and our method for similar actions *Writing* and *Typing on a Keyboard*. Darker colors indicate the stronger correlation between corresponding joints.

existing LLM-based approaches, including LA-GCN [46], GAP [43], and PURLS [57]. In practice, we employ the prompts and action descriptions provided by these methods. As shown in Tab. 4, while their static prompts facilitate the differentiation, the improvement of our method is more significant. This indicates that the agent-based dynamic interaction mechanism can effectively enhance performance.

**Influences of LLMs.** We compare different LLMs for interactions in Tab. 4. Among these models, GPT-4o could provide more discriminative guidance by using our interactive agents, and the generated descriptions achieve the best performance. Additionally, the results demonstrate the robustness of SkeletonAgent when using different LLMs, with performance differences less than 0.6%.

**Effect of Hyper-parameters.** We analyze the effect of the weights  $\alpha$  and  $\beta$  in Fig. 4. The optimal value for  $\alpha$  is determined to be 0.2, corresponding to peak accuracy. In addition, we explore combinations of varying  $\beta$  to balance explicit constraint and implicit alignment. The best overall performance is achieved when  $\beta$  is equal to 0.5.

**Visualization.** To visually demonstrate the effectiveness of SkeletonAgent, we present the related descriptions and the topologies for two similar actions *writing* and *typing on a keyboard* in Fig. 5. The static descriptions are provided by GAP [43], and the topologies are shown by averaging  $\mathbb{R}^{N \times N \times C}$  along the  $C$  dimension. It is observed that previous single-round descriptions lack sufficient contextual information, causing the model to remain constrained to similar hand motions. In contrast, our targeted distinctions leverage dynamic interactions to explicitly highlight key features, guiding the model to concentrate on more dis-

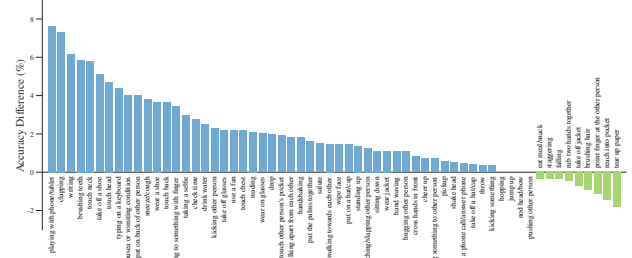


Figure 6. The accuracy difference (%) between our method and PYSKL [10] on the NTU-60 dataset with the joint modality.

criminative single-arm and double-arm motions. The color patterns within topologies reflect that our interaction framework enables the recognition model to effectively focus on crucial differences associated with target motion.

**Performance on Similar Classes.** To demonstrate the superiority of SkeletonAgent in distinguishing similar actions, we present the detailed comparisons in Tab. 5. According to the results of CTR-GCN [3], we split the NTU-60 dataset into three subsets based on difficulty and computed the average accuracy. Specifically, we gather actions whose accuracy is lower than 70% as Hard set, between 70% and 90% as Medium set, and over 90% as Easy set. We compare our method with two other approaches designed to refine similar actions. The experiment is also under the X-Sub setting with the joint modality. The results show that SkeletonAgent consistently improves performance, especially in classes with higher difficulties. The following four rows demonstrate the significant gains achieved by our method on four challenging actions. In addition, Fig. 6 presents the accuracy difference between our method and PYSKL on the NTU-60 dataset. From the comparisons, we can see that SkeletonAgent offers more pronounced improvements in a significantly greater number of classes. These results indicate that our method provides a remarkable advantage in distinguishing confusing action classes.

## 5. Conclusion

In this paper, we introduced SkeletonAgent, a novel interactive framework for skeleton-based action recognition that leverages LLM agents to enable dynamic collaboration between recognition models and language models. Through this multi-turn iterative mechanism, our approach generates targeted discriminative guidance for challenging actions based on continuous feedback from recognition models. The interactive process allows the framework to progressively identify and emphasize crucial fine-grained information, thereby achieving more precise cross-modal alignment between skeletal and semantic representations. Extensive experiments on five benchmark datasets demonstrate the effectiveness of SkeletonAgent, which establishes new state-of-the-art performance across the board.

## References

- [1] Haochen Chang, Pengfei Ren, Haoyang Zhang, Liang Xie, Hongbo Chen, and Erwei Yin. Hierarchical-aware orthogonal disentanglement framework for fine-grained skeleton-based action recognition. In *ICCV*, pages 11252–11261, 2025. 2
- [2] Ma Chang, Junlei Zhang, Zhihao Zhu, Cheng Yang, Yujia Yang, Yaohui Jin, Zhenzhong Lan, Lingpeng Kong, and Junxian He. Agentboard: An analytical evaluation board of multi-turn llm agents. *NeurIPS*, 37:74325–74362, 2024. 2
- [3] Yuxin Chen, Ziqi Zhang, Chunfeng Yuan, Bing Li, Ying Deng, and Weiming Hu. Channel-wise topology refinement graph convolution for skeleton-based action recognition. In *ICCV*, pages 13359–13368, 2021. 6, 7, 8
- [4] Zhan Chen, Sicheng Li, Bing Yang, Qinghan Li, and Hong Liu. Multi-scale spatial temporal graph convolutional network for skeleton-based action recognition. In *AAAI*, pages 1113–1122, 2021. 6
- [5] Ke Cheng, Yifan Zhang, Xiangyu He, Weihang Chen, Jian Cheng, and Hanqing Lu. Skeleton-based action recognition with shift graph convolutional network. In *CVPR*, pages 183–192, 2020. 7
- [6] Hyung-gun Chi, Myoung Hoon Ha, Seunggeun Chi, Sang Wan Lee, Qixing Huang, and Karthik Ramani. Infogcn: Representation learning for human skeleton-based action recognition. In *CVPR*, pages 20186–20196, 2022. 6, 7
- [7] Jeonghyeok Do and Munchul Kim. Skateformer: skeletal-temporal transformer for human action recognition. In *ECCV*, pages 401–420. Springer, 2024. 1, 2, 6
- [8] Yong Du, Wei Wang, and Liang Wang. Hierarchical recurrent neural network for skeleton based action recognition. In *CVPR*, pages 1110–1118, 2015. 2
- [9] Haodong Duan, Jiaqi Wang, Kai Chen, and Dahua Lin. Dg-stgcn: dynamic spatial-temporal modeling for skeleton-based action recognition. *arXiv preprint arXiv:2210.05895*, 2022. 2
- [10] Haodong Duan, Jiaqi Wang, Kai Chen, and Dahua Lin. Pyskl: Towards good practices for skeleton action recognition. In *ACM MM*, pages 7351–7354, 2022. 6, 8
- [11] Haodong Duan, Yue Zhao, Kai Chen, Dahua Lin, and Bo Dai. Revisiting skeleton-based action recognition. In *CVPR*, pages 2969–2978, 2022. 2
- [12] Lin Geng Foo, Tianjiao Li, Hossein Rahmani, Qihong Ke, and Jun Liu. Unified pose sequence modeling. In *CVPR*, pages 13019–13030, 2023. 6
- [13] Zesheng Hu, Zihao Pan, Qiang Wang, Lei Yu, and Shumin Fei. Forward-reverse adaptive graph convolutional networks for skeleton-based action recognition. *Neurocomputing*, 492: 624–636, 2022. 7
- [14] Aaron Hurst, Adam Lerer, Adam P Goucher, Adam Perelman, Aditya Ramesh, Aidan Clark, AJ Ostrow, Akila Welihinda, Alan Hayes, Alec Radford, et al. Gpt-4o system card. *arXiv preprint arXiv:2410.21276*, 2024. 6
- [15] Chao Jia, Yinfei Yang, Ye Xia, Yi-Ting Chen, Zarana Parekh, Hieu Pham, Quoc Le, Yun-Hsuan Sung, Zhen Li, and Tom Duerig. Scaling up visual and vision-language representation learning with noisy text supervision. In *ICML*, pages 4904–4916. PMLR, 2021. 3
- [16] Will Kay, Joao Carreira, Karen Simonyan, Brian Zhang, Chloe Hillier, Sudheendra Vijayanarasimhan, Fabio Viola, Tim Green, Trevor Back, Paul Natsev, et al. The kinetics human action video dataset. *arXiv preprint arXiv:1705.06950*, 2017. 6
- [17] Lipeng Ke, Kuan-Chuan Peng, and Siwei Lyu. Towards to-at spatio-temporal focus for skeleton-based action recognition. In *AAAI*, pages 1131–1139, 2022. 6
- [18] Jidong Kuang, Hongsong Wang, Chaolei Han, and Jie Gui. Zero-shot skeleton-based action recognition with dual visual-text alignment. *PR*, 171(1):1–15, 2025. 1
- [19] Jungho Lee, Minhyeok Lee, Dogyoon Lee, and Sangyoun Lee. Hierarchically decomposed graph convolutional networks for skeleton-based action recognition. In *ICCV*, pages 10444–10453, 2023. 2, 6
- [20] Bo Li, Yuchao Dai, Xuelian Cheng, Huahui Chen, Yi Lin, and Mingyi He. Skeleton based action recognition using translation-scale invariant image mapping and multi-scale deep cnn. In *ICMEW*, pages 601–604. IEEE, 2017. 2
- [21] Sheng-Wei Li, Zi-Xiang Wei, Wei-Jie Chen, Yi-Hsin Yu, Chih-Yuan Yang, and Jane Yung-jen Hsu. Sa-dvae: Improving zero-shot skeleton-based action recognition by disentangled variational autoencoders. In *ECCV*, pages 447–462. Springer, 2024. 1
- [22] Tianjiao Li, Jun Liu, Wei Zhang, Yun Ni, Wenqian Wang, and Zhiheng Li. Uav-human: A large benchmark for human behavior understanding with unmanned aerial vehicles. In *CVPR*, pages 16266–16275, 2021. 6
- [23] Xinyao Liao, Xianfang Zeng, Liao Wang, Gang Yu, Guosheng Lin, and Chi Zhang. Motionagent: Fine-grained controllable video generation via motion field agent. In *ICCV*, pages 11305–11316, 2025. 2
- [24] Dongjingdian Liu, Yan Hu, Kaiwen Hua, Yijing Lu, Zi Zhang, Xiaobo Ma, Zhaoman Zhong, and Pengpeng Chen. Tdsn-gcn: Transformerify overall structure decaying static graph embedding nas-guided gcn for skeleton action recognition. *IEEE TCSVT*, pages 1–14, 2025. 7
- [25] Hongda Liu, Yunfan Liu, Min Ren, Hao Wang, Yunlong Wang, and Zhenan Sun. Revealing key details to see differences: A novel prototypical perspective for skeleton-based action recognition. In *CVPR*, pages 29248–29257, 2025. 2, 6, 7
- [26] Jun Liu, Amir Shahroudy, Mauricio Perez, Gang Wang, Ling-Yu Duan, and Alex C Kot. Ntu rgb+d 120: A large-scale benchmark for 3d human activity understanding. *IEEE TPAMI*, 42(10):2684–2701, 2019. 6
- [27] Jinfu Liu, Xunshun Wang, Can Wang, Yuan Gao, and Mengyuan Liu. Temporal decoupling graph convolutional network for skeleton-based gesture recognition. *IEEE TMM*, 26:811–823, 2023. 7
- [28] Jinfu Liu, Baiqiao Yin, Jiaying Lin, Jiajun Wen, Yue Li, and Mengyuan Liu. Hdbn: A novel hybrid dual-branch network for robust skeleton-based action recognition. In *ICMEW*, pages 1–6. IEEE, 2024. 7

- [29] Ziyu Liu, Hongwen Zhang, Zhenghao Chen, Zhiyong Wang, and Wanli Ouyang. Disentangling and unifying graph convolutions for skeleton-based action recognition. In *CVPR*, pages 143–152, 2020. 6
- [30] Qiguang Miao, Wentian Xin, Ruyi Liu, Yi Liu, Mengyao Wu, Cheng Shi, and Chi-Man Pun. Adaptive pitfall: Exploring the effectiveness of adaptation in skeleton-based action recognition. *IEEE TMM*, 27(1):56–71, 2024. 7
- [31] Alec Radford, Jong Wook Kim, Chris Hallacy, Aditya Ramesh, Gabriel Goh, Sandhini Agarwal, Girish Sastry, Amanda Askell, Pamela Mishkin, Jack Clark, et al. Learning transferable visual models from natural language supervision. In *ICML*, pages 8748–8763. PMLR, 2021. 3, 5, 6
- [32] Fumiaki Sato, Ryo Hachiuma, and Taiki Sekii. Prompt-guided zero-shot anomaly action recognition using pre-trained deep skeleton features. In *CVPR*, pages 6471–6480, 2023. 1
- [33] Amir Shahroudy, Jun Liu, Tian-Tsong Ng, and Gang Wang. Ntu rgb+d: A large scale dataset for 3d human activity analysis. In *CVPR*, pages 1010–1019, 2016. 5
- [34] Dian Shao, Yue Zhao, Bo Dai, and Dahua Lin. Finegym: A hierarchical video dataset for fine-grained action understanding. In *CVPR*, pages 2616–2625, 2020. 6
- [35] Lei Shi, Yifan Zhang, Jian Cheng, and Hanqing Lu. Two-stream adaptive graph convolutional networks for skeleton-based action recognition. In *CVPR*, pages 12026–12035, 2019. 1, 2, 6
- [36] Noah Shinn, Federico Cassano, Ashwin Gopinath, Karthik Narasimhan, and Shunyu Yao. Reflexion: Language agents with verbal reinforcement learning. *NeurIPS*, 36:8634–8652, 2023. 2
- [37] Sijie Song, Cuiling Lan, Junliang Xing, Wenjun Zeng, and Jiaying Liu. An end-to-end spatio-temporal attention model for human action recognition from skeleton data. In *AAAI*, pages 1–7, 2017. 1
- [38] Guy Tevet, Brian Gordon, Amir Hertz, Amit H Bermano, and Daniel Cohen-Or. Motionclip: Exposing human motion generation to clip space. In *ECCV*, pages 358–374. Springer, 2022. 3
- [39] Mengmeng Wang, Jiazheng Xing, Jianbiao Mei, Yong Liu, and Yunliang Jiang. Actionclip: Adapting language-image pretrained models for video action recognition. *TNNLS*, 36(1):625–637, 2023. 3
- [40] Xiaohan Wang, Yuhui Zhang, Orr Zohar, and Serena Yeung-Levy. Videoagent: Long-form video understanding with large language model as agent. In *ECCV*, pages 58–76. Springer, 2024. 2
- [41] Jason Wei, Xuezhi Wang, Dale Schuurmans, Maarten Bosma, Fei Xia, Ed Chi, Quoc V Le, Denny Zhou, et al. Chain-of-thought prompting elicits reasoning in large language models. *NeurIPS*, 35:24824–24837, 2022. 2
- [42] Wenhan Wu, Ce Zheng, Zihao Yang, Chen Chen, Srijan Das, and Aidong Lu. Frequency guidance matters: Skeletal action recognition by frequency-aware mixed transformer. In *ACM MM*, pages 4660–4669, 2024. 2
- [43] Wangmeng Xiang, Chao Li, Yuxuan Zhou, Biao Wang, and Lei Zhang. Generative action description prompts for skeleton-based action recognition. In *ICCV*, pages 10276–10285, 2023. 1, 3, 4, 6, 7, 8
- [44] Jianyang Xie, Yanda Meng, Yitian Zhao, Anh Nguyen, Xiaoyun Yang, and Yalin Zheng. Dynamic semantic-based spatial graph convolution network for skeleton-based human action recognition. In *AAAI*, pages 6225–6233, 2024. 6
- [45] Wentian Xin, Qiguang Miao, Yi Liu, Ruyi Liu, Chi-Man Pun, and Cheng Shi. Skeleton mixformer: Multivariate topology representation for skeleton-based action recognition. In *ACM MM*, pages 2211–2220, 2023. 6, 7
- [46] Haojun Xu, Yan Gao, Zheng Hui, Jie Li, and Xinbo Gao. Language knowledge-assisted representation learning for skeleton-based action recognition. *IEEE TMM*, 27(1):5784–5799, 2025. 1, 3, 7, 8
- [47] Le Xue, Mingfei Gao, Chen Xing, Roberto Martín-Martín, Jiajun Wu, Caiming Xiong, Ran Xu, Juan Carlos Niebles, and Silvio Savarese. Ulip: Learning a unified representation of language, images, and point clouds for 3d understanding. In *CVPR*, pages 1179–1189, 2023. 3
- [48] Sijie Yan, Yuanjun Xiong, and Dahua Lin. Spatial temporal graph convolutional networks for skeleton-based action recognition. In *AAAI*, pages 1–9, 2018. 1, 2, 6
- [49] Zeyuan Yang, Delin Chen, Xueyang Yu, Maohao Shen, and Chuang Gan. Vca: Video curious agent for long video understanding. In *ICCV*, pages 20168–20179, 2025. 2
- [50] Shunyu Yao, Howard Chen, John Yang, and Karthik Narasimhan. Webshop: Towards scalable real-world web interaction with grounded language agents. *NeurIPS*, 35: 20744–20757, 2022. 2
- [51] Jiahang Zhang, Lilang Lin, and Jiaying Liu. Shap-mix: Shapley value guided mixing for long-tailed skeleton based action recognition. *arXiv preprint arXiv:2407.12312*, 2024. 6
- [52] Jiaxu Zhang, Zhigang Tu, Junwu Weng, Junsong Yuan, and Bo Du. A modular neural motion retargeting system decoupling skeleton and shape perception. *IEEE TPAMI*, 46(10): 6889–6904, 2024. 2
- [53] Denny Zhou, Nathanael Schärli, Le Hou, Jason Wei, Nathan Scales, Xuezhi Wang, Dale Schuurmans, Claire Cui, Olivier Bousquet, Quoc Le, et al. Least-to-most prompting enables complex reasoning in large language models. *arXiv preprint arXiv:2205.10625*, 2022. 2
- [54] Huanyu Zhou, Qingjie Liu, and Yunhong Wang. Learning discriminative representations for skeleton based action recognition. In *CVPR*, pages 10608–10617, 2023. 6, 7
- [55] Yuxuan Zhou, Xudong Yan, Zhi-Qi Cheng, Yan Yan, Qi Dai, and Xian-Sheng Hua. Blockgcn: Redefine topology awareness for skeleton-based action recognition. In *CVPR*, pages 2049–2058, 2024. 1, 6
- [56] Youwei Zhou, Tianyang Xu, Cong Wu, Xiaojun Wu, and Josef Kittler. Adaptive hyper-graph convolution network for skeleton-based human action recognition with virtual connections. In *ICCV*, pages 12648–12658, 2025. 2, 6, 7
- [57] Anqi Zhu, Qihong Ke, Mingming Gong, and James Bailey. Part-aware unified representation of language and skeleton for zero-shot action recognition. In *CVPR*, pages 18761–18770, 2024. 1, 7, 8